THE JOURNAL OF BIOLOGICAL CHEMISTRY
Vol. 277, No. 18, Issue of May 3, pp. 16189–16201, 2002
Printed in U.S.A.

Evidence That Arachidonate 15-Lipoxygenase 2 Is a Negative Cell Cycle Regulator in Normal Prostate Epithelial Cells*[S]

Received for publication, December 14, 2001, and in revised form, January 22, 2002
Published, JBC Papers in Press, February 11, 2002, DOI 10.1074/jbc.M111936200

Shaohua Tang‡§, Bobby Bhatia‡§, Carlos J. Maldonado‡, Peiying Yang¶, Robert A. Newman¶, Junwei Liu‡, Dhyan Chandra‡, Jeanine Traag‡, Russell D. Klein‡, Susan M. Fischer‡, Dharam Chopra‖, Jianjun Shen‡, Haiyen E. Zhau, Leland W. K. Chung**, and Dean G. Tang‡ ‡‡**

*From the ‡Department of Carcinogenesis, the University of Texas MD Anderson Cancer Center, Science Park Research Division, Smithville, Texas 78957, the ¶Department of Experimental Therapeutics, University of Texas MD Anderson Cancer Center, Houston, Texas 77030, ‖Institute of Chemical Toxicology, Wayne State University, Detroit, Michigan 48226, and **Molecular Urology and Therapeutics, Department of Urology, Emory University School of Medicine, Atlanta, Georgia 30322*

15-Lipoxygenase 2 (15-LOX2) is a recently cloned human lipoxygenase that shows tissue-restricted expression in prostate, lung, skin, and cornea. The protein level and enzymatic activity of 15-LOX2 have been shown to be down-regulated in prostate cancers compared with normal and benign prostate tissues. The biological function of 15-LOX2 and the role of loss of 15-LOX2 expression in prostate tumorigenesis, however, remain unknown. We report the cloning and functional characterization of 15-LOX2 and its three splice variants (termed 15-LOX2sv-a, 15-LOX2sv-b, and 15-LOX2sv-c) from primary prostate epithelial cells. Western blotting with multiple primary prostate cell strains and prostate cancer cell lines reveals that the expression of 15-LOX2 is lost in all prostate cancer cell lines, accompanied by decreased enzymatic activity revealed by liquid chromatography/tandem mass spectrometry analyses. Further experiments show that the loss of 15-LOX2 expression results from transcriptional repression caused by mechanism(s) other than promoter hypermethylation or histone deacetylation. Subsequent functional studies indicate the following: 1) the 15-LOX2 product, 15(S)-hydroxyeicosatetraenoic acid, inhibits prostate cancer cell cycle progression; 2) 15-LOX2 expression in primary prostate epithelial cells is inversely correlated with cell cycle; and 3) restoration of 15-LOX2 expression in prostate cancer cells partially inhibits cell cycle progression. Taken together, these results suggest that 15-LOX2 could be a suppressor of prostate cancer development, which functions by restricting cell cycle progression.

Lipid signaling molecules markedly modulate prostate tumorigenesis. Animal and epidemiological studies suggest a strong link between fat (in particular, polyunsaturated fatty acids) intake/content in the diet and prostate cancer development and progression (1–3). The major polyunsaturated fatty acids in the human diet is linoleic acid, which is the precursor to arachidonic acid (AA).[1] AA is metabolized via three major biochemical pathways as follows: the cyclooxygenase pathway leading to prostaglandins, prostacyclin, and thromboxane; the lipoxygenase (LOX) pathway giving rise to various hydroperoxy and hydroxy (HETE) fatty acids as well as leukotrienes; and the P450-dependent epoxygenase pathway generating epoxyeicosatrienoic acids. AA itself and many of its metabolites (*i.e.* eicosanoids) are involved in growth-promoting signaling, which may help drive cell proliferation and promote tumor development (4–7). They may also contribute to tumorigenesis by modulating cell death (7–9).

AA is metabolized to a variety of bioactive hydroperoxy and hydroxy fatty acid molecules via LOX. To date at least 18 different LOX sequences have been published, but the biological functions for most of these LOXs remain unknown (10, 11). In human prostate, four LOX molecules, *i.e.* 5-LOX, 12-LOX, 15-LOX1, and 15-LOX2, have been reported at the mRNA, protein, or activity level (12–23). Different LOXs have been proposed to play different contributory roles in prostate tumorigenesis, *e.g.* 5-LOX being a survival factor (12, 13), 12-LOX being a proangiogenic factor (16), and 15-LOX1 somehow affecting p53 functions (18). These three LOXs have been reported to be up-regulated in prostate cancer cells (14, 15, 17, 18), although, in many cases, this correlation has not been corroborated by simultaneous measurement of protein (or mRNA) expression and enzymatic activities.

15-LOX2 is yet another LOX molecule implicated in prostate cancer development. Cloned first by Brash and colleagues (19), 15-LOX2 is most homologous (~80% amino acid identity) to murine 8-LOX and shows only ~40% identity to human 5-LOX, 12-LOX, or 15-LOX1 (19, 20). A splice variant of 15-LOX2 with

* This work was supported in part by NCI Grant CA-90297 (to D. G. T.) from the National Institutes of Health, Burroughs-Wellcome Fund Award BWF-1122 (to D. G. T.), University of Texas MDACC Institutional fund (to D. G. T.), National Institutes of Health Postdoctoral Training Grant T32 CA09480-16 (to C. J. M.), NIEHS Center Grant ES07784 (to D. G. T.) from the National Institutes of Health, and NCI Cancer Center Support Grant CA16672 (to R. A. N.) from the National Institutes of Health. The costs of publication of this article were defrayed in part by the payment of page charges. This article must therefore be hereby marked "*advertisement*" in accordance with 18 U.S.C. Section 1734 solely to indicate this fact.

[S] The on-line version of this article (available at *http://www.jbc.org*) contains Supplemental Fig. 1.

The nucleotide sequence(s) reported in this paper has been submitted to the GenBank™/EBI Data Bank with accession number(s) AF468051–AF468054.

§ Both authors contributed equally to this work.

‡‡ To whom correspondence should be addressed: University of Texas MD Anderson Cancer Center, Science Park Research Division, Park Rd. 1C, Smithville, TX 78957. Tel.: 512-237-9575; Fax: 512-237-2475; E-mail: dtang@sprd1.mdacc.tmc.edu.

[1] The abbreviations used are: AA, arachidonic acid; 15-LOX2, 15-lipoxygenase 2; 15-LOX2sv, 15-lipoxygenase 2 splice variant; BrdUrd, 5-bromo-2′-deoxyuridine; HDAC, histone deacetylase; HETE, hydroxyeicosatetraenoic acid; LC/MS/MS, liquid chromatography/tandem mass spectrometry; LOX, lipoxygenase; NHP, normal human prostate epithelial cells; PFA, paraformaldehyde; RT, reverse transcriptase; GAPDH, glyceraldehyde 3-phosphate dehydrogenase; EGFP, enhanced green fluorescent protein; FBS, fetal bovine serum; PBS, phosphate-buffered saline; GFP, green fluorescent protein; DAPI, 4,6-diamidino-2-phenylindole; PIN, prostate intraepithelial neoplasia; PPAR, peroxisome proliferator-activated receptor.

an in-frame 87-bp deletion has also been reported (20). 15-LOX2 metabolizes exclusively AA to produce 15(S)-hydroxyeicosatetraenoic acid (15(S)-HETE) (19). 15-LOX2 shows an interesting tissue expression pattern, *i.e.* only in prostate, lung, skin, and cornea (19, 20). This tissue-restricted expression pattern suggests that 15-LOX2 may play a role in the normal development of prostate and the other three tissues, and its abnormal expression/function could contribute to tumorigenesis in some of these tissues. Indeed, work by Shappell and co-workers (21, 22) indicates that both 15-LOX2 protein expression and its enzymatic activity are decreased in prostate cancer tissues, and the expression levels of 15-LOX2 are inversely correlated with the pathological grade and Gleason scores of the patients. These findings suggest that 15-LOX2 may normally help maintain the differentiated phenotype of prostate epithelial cells and that loss of 15-LOX2 expression may contribute to prostate cancer development and progression. The major goal of our study is to elucidate the biological functions of 15-LOX2 in normal prostate development as well as in prostate cancer development. In this paper we provide evidence that 15-LOX2 is a negative cell cycle regulator in normal prostate epithelial cells, which may explain why it is advantageous for prostate cancer cells to lose its expression.

MATERIALS AND METHODS

Cells and Reagents—Five normal human prostate (NHP) epithelial cell strains, NHP1–NHP5, were primary cultures freshly isolated from five different donors. TP1 were primary prostate adenocarcinoma cells isolated from the same patient as NHP2 (24–26). NHP1, NHP3, and NHP4 cells were obtained from Clonetics (Walkersville, MD). All these primary strains were cultured in serum-free, PrEBM medium (Clonetics) supplemented with insulin, epidermal growth factor, hydrocortisone, bovine pituitary extract, and cholera toxin (24–26) and used at passage 2–6. PPC-1 cells were isolated from primary prostate carcinoma (27). MDA PCa 2a and 2b cell lines (abbreviated as 2a and 2b, respectively) (28) were derived from primary cultures of bone marrow metastases from a single patient. LNCaP (29), an androgen-responsive cell line and its androgen-independent sublines (C4-2 and C5 (30), PC3 (31), Du145 (32), JCA-1 (33), and Tsu-Pr (34) are all established metastatic cell lines. All cancer cell lines were cultured in RPMI 1640 supplemented with 5% heat-inactivated fetal bovine serum (FBS) and antibiotics. HEK 293 cells, which were used in the transfection experiments, were purchased from ATCC and cultured in Dulbecco's modified Eagle's medium supplemented with 5% FBS and antibiotics.

Rabbit polyclonal anti-5- and −12-LOX and sheep polyclonal anti-15-LOX1 antibodies were obtained from Cayman Chemicals (Ann Arbor, MI). Rabbit polyclonal anti-15-LOX2 antibody (21–23) was purchased from Oxford Biomedical (Rochester, MI). Monoclonal anti-actin and anti-cytochrome *c* antibodies were purchased from ICN (Indianapolis, IN) and BD PharMingen, respectively. A monoclonal anti-BrdUrd (5-bromo-2′-deoxyuridine) antibody (hybridoma culture supernatant) was kindly provided by Dr. Martin Raff. Anti-GFP (green fluorescence protein) antibodies were obtained from CLONTECH (Palo Alto, CA). All secondary antibodies (goat anti-mouse or -rabbit IgG or rabbit anti-sheep IgG conjugated to horseradish peroxidase, fluorescein isothiocyanate, or rhodamine) were acquired from Amersham Biosciences. 15(S)-HETE and other eicosanoids were bought from Cayman Chemicals. All other chemicals were purchased from Sigma unless specified otherwise. Liposome FuGENE 6 was bought from Roche Diagnostics.

Immunohistochemistry of 15-LOX2 Expression in Tissue Sections—Paraffin-embedded sections of normal prostate tissues and prostate cancers were stained by immunohistochemistry using rabbit anti-15-LOX2 and goat anti-rabbit IgG conjugated to alkaline phosphatase followed by substrate 3′3-diamino benzidine (DAB) development. Sections of LNCaP cells grown in nude mice as well as their metastatic variants in bone marrow and lymph node (30) were similarly processed for 15-LOX2 immunostaining.

Immunofluorescence Detection of 15-LOX2 Expression in Cultured Prostate (Cancer) Cells—NHP cells or prostate cancer cells were grown on 13-mm^2 circular glass coverslips. To detect endogenous 15-LOX2 expression in these cells, we used two different permeabilization protocols. Specifically, following fixation in 4% paraformaldehyde (PFA) at 4 °C for 1 h, cells were permeabilized with either 1% Triton X-100 in PBS for 20 min or −20 °C acidic alcohol (95% ethanol, 5% glacial acetic acid) for 10 min. After washing, coverslips were blocked in 30% goat whole serum followed by incubation in primary antibody (1:2000 dilution of anti-15-LOX2) and secondary antibody (goat anti-rabbit IgG-fluorescein isothiocyanate; 1:2000). Finally, cells were incubated with 1 μg/ml propidium iodide to label all nuclei. After extensive washing, coverslips were mounted on slides using Vectorshield mounting medium (Vector Laboratories, Inc., Burlingame, CA) and observed under an Olympus BX40 epifluorescence microscope. Images were captured with MagnaFire software and processed in Adobe Photoshop.

Western Blotting—Whole cell lysates were prepared in complete RIPA buffer (50 mM Tris-HCl, pH 7.5, 150 mM NaCl, 1% Nonidet P-40, 0.5% sodium deoxycholate, 0.5% Triton X-100, 10 mM EDTA) containing protease inhibitor mixture. Protein concentrations were determined by MicroBCA kit (Pierce). Various amounts of proteins were loaded on a 15% SDS-PAGE. Western blotting was performed as described previously (8, 26) using ECL.

Determination of 15-HETE Production in Prostate (Cancer) Cells by LC/MS/MS—The enzymatic activities of 15-LOX2 in normal and cancerous prostate cells were analyzed with LC/MS/MS using the modified procedure described by Kempen *et al.* (35). Briefly, log-phase NHP1, NHP3, LNCaP, PC3, and DU145 were harvested with trypsinization, and cell pellets were washed in 5 ml of PBS and resuspended in 0.5 ml of PBS with 1 mM calcium chloride solution. Cell suspension (1×10^7/ml) was incubated at 37 °C for 2 min. Then an aliquot of 2.5 μl of calcium ionophore A23187 (1 mM) was added, followed by the addition of 100 μM of AA. The reaction mixture was incubated at 37 °C for 10 min at minimum light. At the end of incubation, 40 μl of 1 N citric acid, 5 μl of 1% butylated hydroxytoluene, and 20 μl of 15-HETE-d_8 (internal standard) were added to the samples. The lipids were extracted from the reaction mixture three times with 2 ml of hexane:ethyl acetate (1:1). Organic phases were collected and dried under a stream of nitrogen. Samples were reconstituted in 200 μl of methanol, 10 mM ammonium acetate, pH 8.5 (70:30), and analyzed using LC/MS/MS. Reverse-phase high pressure liquid chromatography and mass spectrometry was performed using a Quattro Ultima tandem mass spectrometer (Micromass, Beverly, MA) equipped with an Agilent HP1100 binary pump high pressure liquid chromatography inlet. Eicosanoid metabolites were separated using a YMC ODS-AQ 2.0 × 100-mm column (S3 μm, 120 Å, Waters Associates). Mobile phases consisted of 10 mM ammonium acetate, pH 8.5 (phase A) and methanol (phase B). Flow rate was 250 μl/min with column maintained at 40 °C. Sample injection volume was 25 μl. The mass spectrometer was operated in electrospray negative ion mode with a cone voltage of 100, source temperature of 120 °C, and collision cell pressure of 2.10×10^{-3} torr using argon as collision gas. The collision energy was 19 V. A minimum of duplicate samples was measured in each experiment, and experiments were repeated three times. The results were expressed as nanograms of 15(S)-HETE/5×10^6 cells pooled from three independent experiments.

RT-PCR Analysis of 15-LOX2 mRNA Expression—Total RNA and mRNA were isolated using Tri-reagent (Invitrogen) and Poly(A)Pure kit (Ambion, Austin, TX), respectively, according to the manufacturers' instructions. Either 2 μg of total RNA or 0.5 μg of mRNA from each cell type was used in RT (42 °C × 2 h) in a total of 20 μl reaction containing random hexamers and Superscript II reverse transcriptase (Invitrogen). Two pairs of PCR primers were designed based on the published 15-LOX2 cDNA sequence (19; GenBank™ accession number U78294). Primers A (sense, 5′-AACTCACCCCCACCACCATACACA-3′) and B (antisense, 5′-TTCCCGCCTCCATCTCCCAAAGT-3′) cover nucleotides 2234–2584 in the 3′-untranslated region (3′-untranslated region) of 15-LOX2. Primers C (sense, 5′-ACTACCTCCCAAAGAACTTCCCC-3′) and D (antisense, 5′-TTCAATGCCGATGCCTGTG-3′) cover nucleotides 835–1379 in the 15-LOX2 coding region. For PCR, 2 μl of cDNA from each cell type was used in a 25-μl reaction containing 0.5 μM primers, dNTPs, *Taq*, using the cycling profile 94 °C for 30 s, 60 °C for 45 s, and 72 °C for 1 min for 35 cycles. PCR products were analyzed by agarose gel electrophoresis. RT-PCR of glyceraldehyde-3-phosphate dehydrogenase (GAPDH) was used as a control (36).

Northern Blotting—One μg of mRNA from each cell type (*i.e.* NHP3, NHP4, PPC-1, JCA-1, LNCaP, C4–2, and PC3) was fractionated on a 1.5% formaldehyde-agarose gel. Following alkaline hydrolysis, RNA was transferred to Hybond$^+$ membrane (Amersham Biosciences) followed by UV cross-linking. After prehybridization in ExpressHyb solution (CLONTECH) for 1 h, the membrane was hybridized to a ^{32}P-labled 15-LOX2 cDNA probe overnight at 55 °C. The probe used was a 759-bp *Egl*I fragment (from nucleotide 43 to 802), and the probe was labeled using Ready-to-Go labeling kit (Amersham Biosciences). Following hybridization, the membrane was washed twice (30 min each) at 50 °C in 2× SSC buffer containing 0.1% SDS, followed by washing twice (30 min

each) in 0.1× SSC buffer containing 0.1% SDS. Then the membrane was stripped and rehybridized to a ^{32}P-labeled β-actin cDNA probe.

Treatment with Inhibitors of DNA Methylation and Histone Deacetylation (HDAC)—Log-phase LNCaP, PC3, and Du145 cells (50–60% confluence) were treated with 5′-azadeoxycytidine (3 μM), which inhibits DNA methyltransferase (37), or trichostatin A (0.5 μM), which inhibits HDAC (38, 39), or both for 7 days with fresh media changed and drugs re-added on the 3.5 day. At the end of the treatment, cells were harvested either to prepare proteins for Western blotting or to prepare total RNA for RT-PCR using C-D primers.

Cloning of 15-LOX2 and Splice Variants—We first cloned out two large 15-LOX2 fragments from NHP2 and TP1 cells. cDNA was synthesized from total RNA using the SMART cDNA synthesis kit (CLONTECH) according to the manufacturer's instructions and PCR-amplified. 15-LOX2 fragments G-H (nucleotide 1880–2638) and I-J (nucleotides 131–2253) were amplified using primers G (sense, 5′-CATCCTTGCTCTCTGGTTGC-3′) and H (antisense, 5′-TGGAGTCTCGCTATGTCGTC-3′), and I (sense, 5′-CAAAGTGTCTGTCAGCATCGTGG-3′) and J (antisense, 5′-TATGGTGGTGGGGGTGAGTTAC-3′), respectively. Subsequently, we cloned the full-length 15-LOX2 and its splice variants using PCR-based strategies. cDNA synthesis and PCR amplification were carried out using a SuperScript One-step long distance PCR kit (Invitrogen), using 1 μg of NHP2 mRNA and several more pairs of cloning primers. Primers CP-5′ (sense, GCTAGCCTGGCAGCATGGCCGAGTTCAG-3′) and CP-3′ (antisense, CTCGAGGATGGAGACGCTGTTCTCG-3′) cover the entire coding region (nucleotides 64–2099) from the translation-initiation codon/Kozak sequence to the sequence immediately in front of TAA stop codon, with the *Nhe*I and *Xho*I restriction enzyme sites incorporated to the 5′-ends of the primers, respectively. Primers K (sense, TGCGCCGTAGAGAGCTGGACTT-3′) and H (see above) cover nearly the whole published 15-LOX2 sequence from nucleotides 36 to 2638. mRNA was denatured at 65 °C for 5 min and then mixed with the buffer containing various enzymes. Then coupled cDNA synthesis and PCR amplification were carried out at 50 °C for 30 min followed by 94 °C for 3 min and then 94 °C for 15 s, 55 °C for 30 s, and 68 °C for 4 min for 40 cycles, using either CP-5′/CP-3′ or K/H primer pairs. Following PCR amplification, all distinct bands were excised and cloned into pCRII-TOPO (Invitrogen). Colonies were screened using a combination of PCR with C and D primers and restriction digestion with *Eco*RI. Multiple positive colonies of different sizes of inserts as well as various PCR fragments were sequenced from both directions and characterized.

Construction and Characterization of Expression Vectors of 15-LOX2 and Its Splice Variants—Full-length 15-LOX2 and its splice variants were re-amplified from pCRII-TOPO vectors using *Pfu* Turbo DNA polymerase (Stratagene, La Jolla, CA) and primers CP-5′ and CP-3′ with TTA stop codon added in the CP-3′ primer. Individual products were recloned into pCRII-TOPO vector, and the *Eco*RI fragments containing the full-length molecules were subcloned into pCMS-EGFP vector (CLONTECH), in which EGFP and target genes are driven by separate promoters. Alternatively, the K-H fragments were directly released from pCRII-TOPO with *Eco*RI and then subcloned into pCMS-EGFP. The resultant expression vectors were subjected to restriction mapping as well as sequencing to determine the orientation of expression.

To characterize these vectors, which we have designated pEGFP-15LOX2, pEGFP-15LOX2sv-a, pEGFP-15LOX2sv-b, and pEGFP-15LOX2sv-c, respectively, we first transfected them into HEK 293 cells using FuGENE 6. Seventy two h later, cells were harvested for either Western blotting or LC/MS/MS determination of 15(S)-HETE production.

Effect of Exogenous 15(S)-HETE on Cell Proliferation and Survival—NHP2, TP1, LNCaP, PC3, and Du145 cells were plated in 24-well culture plates at 1×10^4 cells/well. The next day, cells were treated with 15(S)-HETE at 0.1, 1, 10, 25, 50, and 75 μM. Seventy two h later, cells were harvested, and the number of live and dead cells was determined using trypan blue dye exclusion assays (8). Each condition was run in quadruplicate, and the results are expressed as the mean percentage cell number (relative to vehicle (ethanol) control) ± S.E. obtained from three repeat experiments.

To determine whether inhibition of cell proliferation was caused by inhibition of cell cycle progression, we performed BrdUrd incorporation experiments. Various cells were plated on glass coverslips and treated with 15(S)-HETE for 72 h, similarly as described above. During the last 6 h, BrdUrd (10 μM final concentration) was added, and cells were then processed for BrdUrd immunostaining, using the protocol we established previously (36). Briefly, at the end of BrdUrd pulse, cells were fixed in PFA and permeabilized in acidic alcohol, and DNA was denatured in acidic HCl. Then cells were incubated with the monoclonal anti-BrdUrd antibody followed by goat anti-mouse IgG conjugated to fluorescein isothiocyanate. Cells were counterstained with bisbenzimide (Hoechst 33342) or DAPI. An average of 500–1000 cells were counted for each cell type, and the results were expressed as % BrdUrd$^+$ cells (36, 40).

Studies on 15-LOX2 Expression and Cell Cycle in NHP Cells—We first used immunofluorescent staining to assess the relationship between 15-LOX2 expression and cell cycle. Log-phase NHP1 or NHP2 cells grown on glass coverslips (1×10^4 cells/13 mm^2) were pulsed with BrdUrd (10 μM) for 4 h followed by double labeling of 15-LOX2 and BrdUrd, basically using the protocol described above for 15-LOX2 and BrdUrd staining alone. An average of 200–1000 cells was counted, and the results are expressed as percentage of BrdUrd$^+$ cells in the total number of 15-LOX2$^+$ and 15-LOX2$^-$ cells.

To study further the relationship between 15-LOX2 expression and cell cycle progression, cell cycle arrest was induced in NHP2 cells by subjecting them to growth factor deprivation for 1 day. In another experiment, starved NHP2 cells were re-cultured in factor-containing medium for 1 day (*i.e.* release 1 day). At the end, cells were fixed and used for 15-LOX2-BrdUrd double labeling.

Restoration of 15-LOX2 Expression in Prostate Cancer Cells—PC3 or PPC-1 cells grown on glass coverslips (3×10^3 cells/13 mm^2) were either untransfected or transiently transfected with empty vector (*i.e.* pCMS-EGFP), pEGFP-15LOX2, or its splice variants (1 μg of plasmid/coverslip) with FuGENE 6. Seventy two h later, cells were pulsed with 10 μM BrdUrd for the final 4 h and then processed for BrdUrd immunostaining using a modified protocol. Briefly, cells were first fixed in 4% PFA at 4 °C for 1 h to preserve GFP, followed by permeabilization in 1% Triton X-100 for 20 min at room temperature. To denature DNA, we incubated cells with 100 μg/ml DNase in PBS containing 1% Triton for 90 min at room temperature instead of the regular HCl step, which destroys the GFP signal. Then cells were stained for BrdUrd, as described above. The results were expressed as % BrdUrd$^+$ cells of the total number of GFP$^+$ and GFP$^-$ cells. Two individuals independently counted an average of 600–1500 cells for each condition, and experiments were repeated three times.

To confirm the 15-LOX2 expression in transfected cells, immunostaining with anti-15-LOX2 antibody was performed. We also developed a double labeling, tri-color fluorescence protocol that allowed us to monitor simultaneously 15-LOX2 expression and BrdUrd incorporation in GFP$^+$ cells. Briefly, 72 h after transfection with control vector or various 15-LOX2 expression vectors, cells were pulsed with BrdUrd (10 μM; 4 h) and then fixed cells in 4% PFA followed by permeabilization in 1% Triton. Cells were then stained for 15-LOX2 using the rabbit polyclonal anti-15-LOX2 followed by goat anti-rabbit IgG conjugated to Texas Red. Finally, cells were processed for BrdUrd using monoclonal anti-BrdUrd followed by goat anti-mouse IgG conjugated to Cascade Blue (Molecular Probes, Eugene, OR), which was observed using the DAPI bandpass.

RESULTS

15-LOX2 Protein Expression Is Lost in all Prostate Cancer Cells Examined—15-LOX2 was recently shown to be down-regulated/lost in prostate cancer tissues (21, 22). We first sought to confirm this independently. An immunohistochemical analysis with a small sample size (1 normal, 1 prostate intraepithelial neoplasia (PIN), and 4 prostate cancer sections), using the same rabbit polyclonal anti-15-LOX2 antibody (21, 22), revealed that 15-LOX2 was indeed abundantly expressed in normal prostate epithelia, greatly reduced in PIN, and completely lost in prostate cancer tissues (see Supplemental Material, Fig. 1). Our data, therefore, support the previous observations by Shappell and co-workers (21, 22). A similar immunohistochemical staining for 15-LOX2 on sections of LNCaP and its metastatic variants (30) grown in nude mice also did not reveal any positive staining (not shown).

To circumvent certain inherent pitfalls associated with studies using tissues or tissue sections (*e.g.* correlative nature, mixed tumor, and host cells and difficulties in performing biochemical/molecular characterizations and establishing the cause-and-effect relationship), we chose to study early passage (*i.e.* 2–6) primary prostate epithelial cells in an attempt to understand the biological functions of 15-LOX2. We first per-

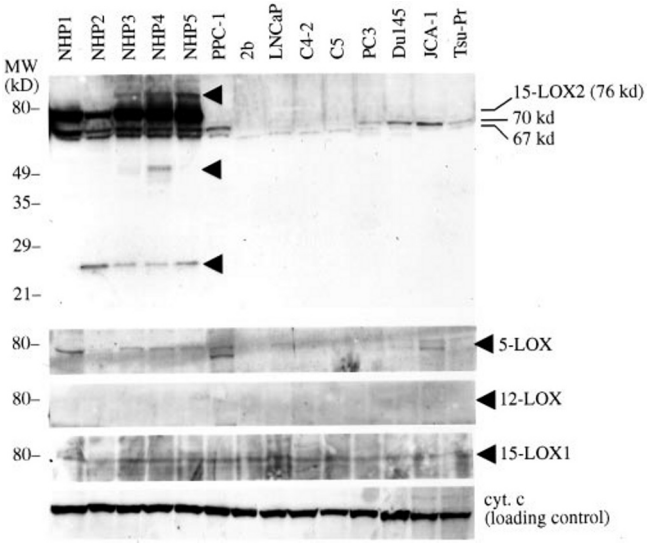

FIG. 1. **15-LOX2 protein expression is lost in prostate cancer cells.** Whole cell lysates (50 μg) from each cell type were separated by 15% SDS-PAGE. The membrane was first probed with the polyclonal anti-15-LOX2 and then stripped and reprobed with the antibodies against the molecules indicated. Cytochrome *c* (*cyt. c*) was used as the loading control. 15-LOX2 and two lower bands are indicated on the *right*. The molecular mass markers are indicated on the *left*. *Arrowheads*, additional bands detected only in NHP cells but not in prostate cancer cells. Note that no 12-LOX band was detected.

formed Western blotting analysis of 15-LOX2 expression using 5 primary strains of normal human prostate (NHP1–5) epithelial cells and 9 established prostate cancer cell lines. As shown in Fig. 1, all 5 NHP strains expressed abundant ~76-kDa 15-LOX2 protein, whereas none of the cancer cells expressed the protein. In addition to 15-LOX2, we also detected two lower bands migrating at ~70 and ~67 kDa, respectively, which were significantly reduced in all prostate cancer cells (Fig. 1). Furthermore, at least one upper band (~83 kDa) and two lower bands (~52 and 26 kDa, respectively) were observed specifically in NHP but not in cancer cells (Fig. 1, *arrowheads*).

In contrast to 15-LOX2, 15-LOX1 was expressed at low levels in all cells examined (Fig. 1). 5-LOX was expressed at variable levels in these cells, and it was, in general, reduced in prostate cancer cells (Fig. 1). We could not detect 12-LOX in any of these cells, even at 150 μg/lane protein loading (Fig. 1 and not shown).

Loss of Expression of 15-LOX2 in Prostate Cancer Cells Leads to Significantly Reduced 15(S)-HETE Production—The above Western blotting data are consistent with our immunohistochemical results (Supplemental Material, Fig. 1) and the results of others (21, 22). To determine whether loss of 15-LOX2 expression would result in reduced enzymatic activity in prostate cancer cells, we measured 15(S)-HETE production in several NHP and prostate cancer cells using LC/MS/MS. As shown in Table I, the 15(S)-HETE production in prostate cancer cells (LNCaP, PC3, and Du145) was indeed much lower (~10-fold decrease) than in NHP (*i.e.* NHP1 and NHP3) cells.

Loss of 15-LOX2 Expression in Prostate Cancer Cells Occurs at the mRNA Level—To explore the mechanism(s) underlying the loss of 15-LOX2 protein expression in prostate cancer cells, we carried out RT-PCR analyses and Northern blotting (Fig. 2). RT-PCR using primers A and B in the 3′-untranslated region detected abundant 15-LOX2 mRNA in all 5 NHP strains but detected little or no message in prostate cancer cells (Fig. 2*a*, *upper panel*). Similarly, RT-PCR using primers C and D in the 15-LOX2 coding region detected the expected 545-bp 15-LOX2 band in all NHP cells, which was not detected or only faintly

TABLE I
15(S)-HETE production in primary prostate epithelial cells and prostate cancer cells

15(S)-HETE production was measured in log phase cells using LC/MS/MS analysis as detailed in the text. Data were obtained from three independent experiments, and the values are mean ± S.D. derived from six samples with each cell type (n = 6).

Cell	15(S)-HETE level
	ng/5 × 10^6 cells
NHP1	28.47 ± 0.96
NHP3	29.02 ± 1.26
LNCaP	2.56 ± 0.38
PC3	3.94 ± 0.28
Du145	3.22 ± 0.26

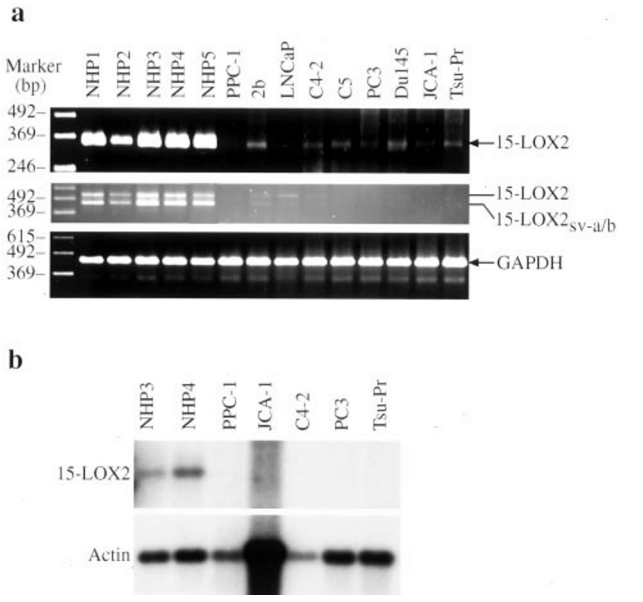

FIG. 2. **15-LOX2 mRNA expression is reduced or lost in prostate cancer cells.** *a*, RT-PCR analysis of 15-LOX2 mRNA expression in NHP and prostate cancer cells. *Upper panel*, PCR using A-B primer pair (see "Materials and Methods"). The expected 15-LOX2 product is 351 bp. *Middle panel*, PCR using C-D primer pair. The expected 15-LOX2 product is 545 bp (the *upper band*), and the 15-LOX2sv-a/15-LOX2sv-b band is ~460 bp (the *lower band*). Note that the *middle panel* was underexposed to clearly show the two bands. *Lower panel*, PCR of GAPDH. *b*, Northern blotting. *Upper panel*, 15-LOX2. *Lower panel*, β-actin.

seen in prostate cancer cells (Fig. 2*a*, *middle panels*, *upper band*). Both the A-B band and the C-D upper band were confirmed to be 15-LOX2 by sequencing the PCR fragments. RT-PCR using primers C-D also detected a lower band of 459 bp in NHP cells (Fig. 2*a*, *middle panel*, *lower band*). This band represents both 15-LOX2 splice variants a and b (15-LOX2sv-a *and* 15-LOX2sv-b, respectively), which could not be distinguished from each other because they have the same splicing structure in the region covered by primers C and D (see below).

Northern blotting similarly detected the ~2.6-kb 15-LOX2 mRNA in NHP cells but not in prostate cancer cells (Fig. 2*b*). We could not detect the alternatively spliced 15-LOX2 isoforms, even in NHP cells (Fig. 2*b*), probably because their mRNA levels are too low.

The above results together suggest that loss of 15-LOX2 protein expression in prostate cancer cells results from transcriptional repression or mRNA instability.

Loss of 15-LOX2 Expression in Prostate Cancer Cells Is Caused by Mechanisms Other Than Promoter (Gene) Hypermethylation or Histone Deacetylation-induced Chromatin Overcompaction—Transcriptional repression or silencing of genes in many cases results from epigenetic changes, especially pro-

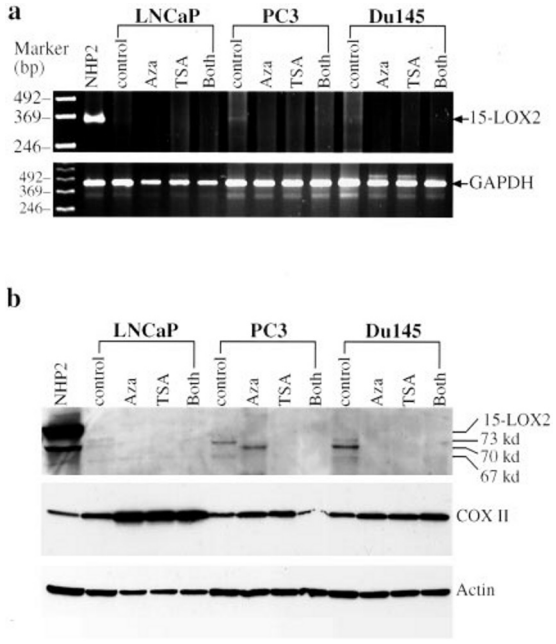

FIG. 3. **Inhibitors of DNA methylation or histone deacetylation could not induce the re-expression of 15-LOX2 mRNA (*a*) or protein (*b*) in prostate cancer cells.** LNCaP, PC3, and Du145 cells were treated with either vehicle ethanol (*control*), 5′-azadeoxycytidine (*Aza*), or trichostatin A (*TSA*) either individually or in combination (*Both*) as detailed under "Materials and Methods." Untreated NHP cells were used as positive control. *a*, RT was performed with 2 μg of total RNA from each condition using random hexamers, and PCR was performed using 2 μl of cDNA and primers A and B. RT-PCR of GAPDH was used as control. *b*, 60 μg/lane protein was separated by 10% SDS-PAGE and then used in Western blotting for 15-LOX2. The membrane was stripped and re-probed with a monoclonal anti-cytochrome *c* oxidase subunit II (*COX II*) (*middle panel*) or anti-actin (*lower panel*).

moter hypermethylation or chromatin compaction due to histone deacetylation or both, for example (37, 39). To test whether these mechanisms may explain, at least partially, the loss of 15-LOX2 expression in prostate cancer cells, we treated LNCaP, PC3, and Du145 cells with 5′-azadeoxycytidine, which inhibits DNA methyltransferase (37), or trichostatin A, which inhibits HDAC (38, 39), either individually or in combination and then analyzed 15-LOX2 mRNA and protein expression. As shown in Fig. 3, these treatments did not lead to the re-expression of 15-LOX2 mRNA (Fig. 3*a*, *upper panel*) or protein (Fig. 3*b*, *upper panel*). By contrast, both 5′-azadeoxycytidine and TSA were effective in up-regulating the maternally inherited mitochondrial gene, cytochrome *c* oxidase subunit II (41), especially in LNCaP cells (Fig. 3*b*, *middle panel*). Treatment of NHP2 cells with these two inhibitors did not affect the endogenous 15-LOX2 expression (not shown). Together, these data suggest that mechanisms other than hypermethylation and histone deacetylation are responsible for the silencing of 15-LOX2 (*ALOX15B*) gene in prostate cancer cells.

NHP Cells Express Multiple 15-LOX2 Splice Variants—To understand better the biological functions of 15-LOX2, we decided to clone out the full-length 15-LOX2 and any apparent splice variants. We adopted a one-step RT-PCR cloning strategy for this purpose. As shown in Fig. 4*a*, using primers CP-5′ and CP-3′ that cover the full coding sequence of 15-LOX2, we detected the expected ~2.0-kb 15-LOX2 in NHP3 cells. In addition, one distinct upper band (~2.1 kb) and 2 lower bands (1.94 and ~1.8 kb, respectively), which may represent 15-LOX2 splice variants, were also detected in NHP3 cells (Fig. 4*a*). The same expression pattern was also observed in NHP2 cells (not shown). All these bands were greatly reduced in primary carcinoma TP1 cells and undetectable in PPC-1, PC3, and LNCaP C4–2 cells (Fig. 4*a*). As expected, TP1 cells expressed barely detectable 15-LOX2 protein (not shown). When we used the K and H primers that cover nearly the full length of 15-LOX2 cDNA (see "Materials and Methods") to perform the PCR cloning, we observed more upper and lower bands in addition to the expected 15-LOX2 band in NHP2 but not in cancer cells (not shown).

We subsequently cut out several bands and cloned out, from NHP2 cells, the full-length 15-LOX2 and three of its splice variants. Eight sequence variants that were different from the published 15-LOX2 cDNA sequence (19) were identified. Six of these sequence variants, *i.e.* 561(A/G) (numbering from ATG), 921(G/T), 1440(T/C), 1584insA, 1587delT, and 1650(A/C), were silent nucleic acid changes. The other two, 811(T/G) and 1457(G/A), resulted in conserved amino acid changes, *i.e.* L270V and R486H, respectively. Interestingly, another sequence variant, L271V, was described previously (20). The sequence variants reported here were found in 100% of our clones (>20) sequenced. They might represent rare sequence differences in our sample (*i.e.* prostate-specific 15-LOX2) or true polymorphisms. In NHP cells, there are at least three 15-LOX2 splice variants, which we named 15-LOX2sv-a, 15-LOX2sv-b, and 15-LOX2sv-c, respectively (Fig. 4 and Table II). In 15-LOX2sv-a, exon 9 (87 bp) was spliced out, generating a protein of 647 amino acids with an estimated molecular mass of ~73 kDa (Table II and Fig. 4*d*). This splice variant is identical to the 15-LOX2 splice variant reported previously (20; GenBank™ accession number AF149095). In 15-LOX2sv-b, in addition to exon 9 being spliced out, another splicing event took place between nucleotides 1516 and 1650, removing part of exon 10 and the entire exon 11 (Fig. 4*d* and Table II). This splice variant is predicted to encode a 602-amino acid protein with an estimated molecular mass of ~67 kDa. When performing RT-PCR using primers C and D that covers nucleotides 835–1379, both 15-LOX2sv-a and 15-LOX2sv-b would be detected as an ~459-bp fragment (see Fig. 2*a, middle panel, lower band*), because both variants have exon 9 spliced out. In 15-LOX2sv-c, intron 12 (80 bp) was retained, generating a molecule of ~2.1 kb in coding region, which was the biggest in the four 15-LOX2 molecules we cloned (Fig. 4*b*). However, the retention of intron 12 resulted in a frameshift and premature stop codon and led to a protein of 617 amino acids with an estimated molecular mass of ~70 kDa (Fig. 4*d* and Table II).

To characterize these splice variants, we subcloned 15-LOX2 and its splice variants into a binary expression vector pCMS-EGFP, in which EGFP and target genes are driven by different promoters. When we transiently transfected 15-LOX2 and its splice variants into HEK 293 cells, we detected the protein bands of the expected molecular weight in the transfected cells (Fig. 4*c*). In subsequent biological studies, we focused on 15-LOX2 and 15-LOX2sv-a, both of which had been well characterized before (19, 20). We are currently performing further biochemical characterizations of 15-LOX2sv-b and 15-LOX2sv-c, and the results will be reported elsewhere.

15-LOX2 Product, 15(S)-HETE, Demonstrates More Pronounced Inhibitory Effects on the Proliferation/Survival of Prostate Cancer Cells Than NHP Cells—To understand the biological functions of 15-LOX2, we first analyzed the effect of its product, 15(S)-HETE, on the proliferation and survival of normal (NHP2), primary carcinoma (TP1), and metastatic (LNCaP, PC3, and Du145) prostate cancer cells. As shown in Table III and Fig. 5*a*, exogenous 15(S)-HETE, in a concentration-dependent manner, reduced cell number, especially in prostate cancer cells. At concentrations <25 μM, there was no obvious cell death in any cell type, but, at ≥25 μM, 15(S)-HETE induced

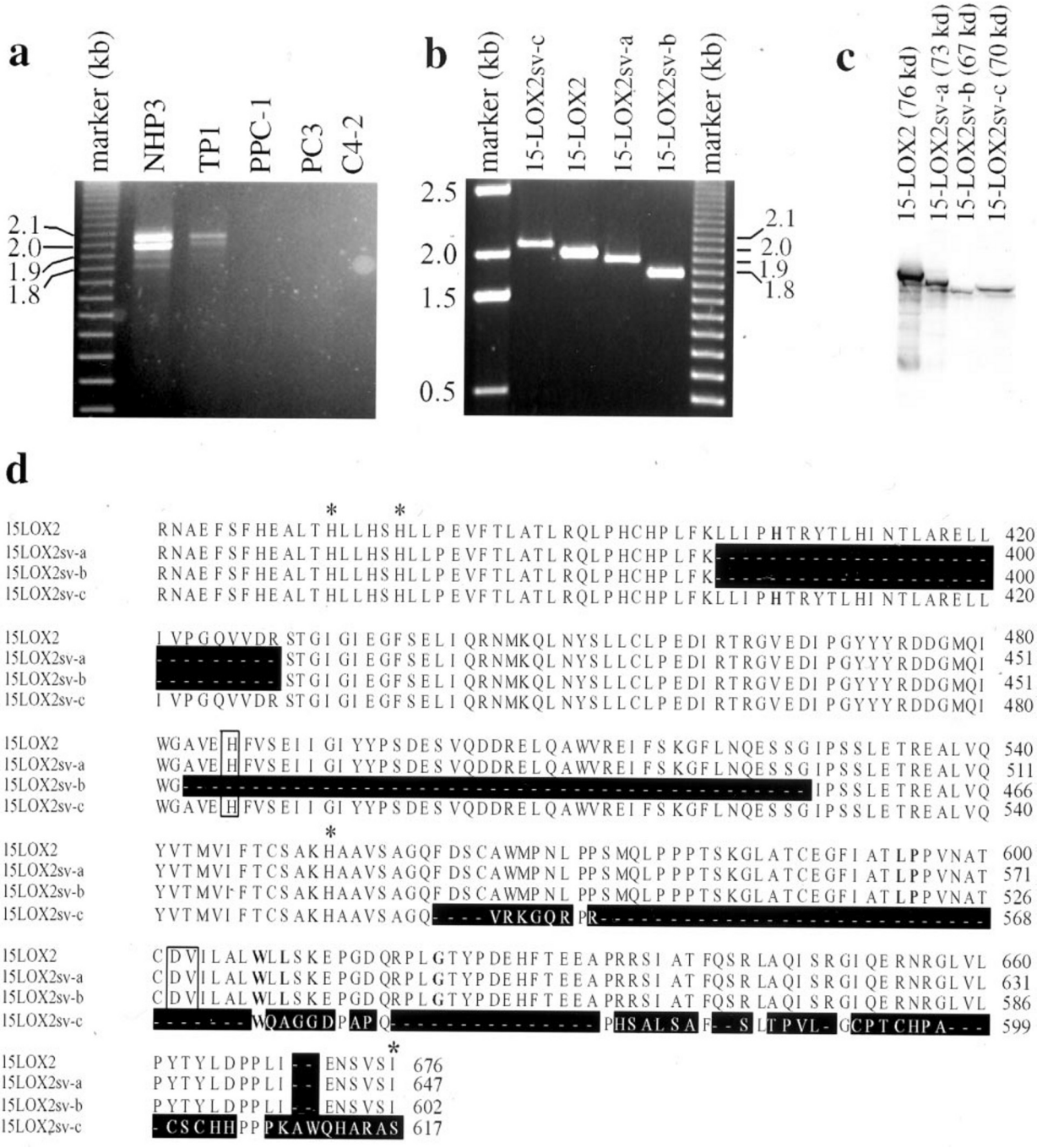

FIG. 4. **Cloning and characterization of 15-LOX2 and its splice variants.** *a*, RT-PCR analysis of 15-LOX2 expression. mRNA (0.5 μg) from each cell type indicated was used in a one-step RT-PCR protocol using primers CP-5′ and CP-3′ (see "Materials and Methods") that cover the full coding sequence of 15-LOX2. For comparative purposes, primary carcinoma cells TP1 and three cancer cell lines, PPC-1, PC3, and C4–2, were also included. The molecular weight markers are indicated at the *left*. Note that NHP3 cells showed four bands, whose intensities were greatly reduced in TP1 cells and lost in the three prostate cancer cell lines. *b*, the cloned products of 15-LOX2 and its splice variants. *c*, Western blotting of 15-LOX2 and its splice variants in HEK 293 cells transiently transfected (72 h) with respective expression constructs. *d*, amino acid sequence alignment using MegAlign program Clustal algorithm with PAM250 residue weight table. Only the divergent sequences corresponding to amino acids 361–676 of 15-LOX2 are shown. The divergent parts are highlighted by *dark boxes.* Several amino acids conserved in all mammalian LOXs are in *bold*. The three His residues (*i.e.* His^{373}, His^{378}, and His^{553} that correspond to His^{361}, His^{366}, and His^{553} of the rabbit reticulocyte 15-LOX; see Ref. 10) and the C-terminal Ile residue important in coordinating iron are marked by *asterisks.* The Asp^{602}–Val^{603} sequences important for determining 15-LOX2 substrate specificity as well as the R486H are *boxed*. See text for detailed discussions.

concentration-related apoptosis, as judged by morphology and DNA fragmentation assays (not shown). Interestingly, the 15(S)-HETE effect was more pronounced in prostate cancer cells than in NHP cells (Table III). For example, at 10 μM, 15(S)-HETE inhibited prostate cancer cell proliferation by 30–50%; however, it had only a marginal effect on NHP2 cells (Table III). At 75 μM 15(S)-HETE, all cancer cells died but ~30% of NHP2 cells survived. We determined the IC_{50} values of 15(S)-HETE inhibition of cell proliferation/survival to be ~50, 25, 25, 25, and 10 μM for NHP2, TP1, LNCaP, PC3, and Du145 cells, respectively (Table III).

15(S)-HETE at <25 μM exerted a concentration-dependent inhibitory effect on prostate cancer cells without inducing apoptosis, suggesting that, at the lower doses, 15(S)-HETE prob-

TABLE II
Exon-intron compositions of 15-LOX2 and splice variants

The 15-LOX[2] exon-intron relationship was deduced based on GenBank data U78294 (cDNA sequence), AJ305028 (exons 1–3), AJ305029 (exons 4–5), AJ305030 (exons 6–8), and AJ305031 (exons 9–14).

Exon	cDNA position[a]	Splice acceptor[b]	Splice donor[b]	Intron[c]
bp				*bp*
1 (153)	72–224		GAGGAG/**gt**gcgt	1 (85)
2 (214)	225–438	gagg**ag**/GACTTC	GTACAG/**gt**gagg	2 (296)
3 (82)	439–520	ccac**ag**/CCAAGG	GTACCA/**gt**gagg	3 (>500)
4 (123)	521–643	ctcc**ag**/GTGGAA	CTCTGC/**gt**gagg	4 (289)
5 (104)	644–747	tggc**ag**/TTTTGC	CAGCTG/**gt**gagg	5 (>570)
6 (173)	748–920	ctgc**ag**/AGCACG	CTAGAG/**gt**gagg	6 (235)
7 (147)	921–1067	ctgc**ag**/AAGGGC	ATCCAG/**gt**atgc	7 (98)
8 (204)	1068–1271	cccc**ag**/CTCAGC	TTCAAG/**gt**cagt	8 (981)
9 (87)	1272–1358	atgc**ag**/CTGCTG	GACAGG/**gt**gaga	9 (152)
**sv-a*/*sv-b*	*exon 9 spliced out*			
10 (170)	1359–1528	tctc**ag**/TCCACA	GGAACG/**gt**gagg	10 (180)
**sv-b*	*1516–1650 spliced out*		*TTTGGG*/***gt****gcag*	
11 (122)	1529–1650	ttgc**ag**/CTTTGT	GCTCAG/**gt**acag	11 (184)
12 (101)	1651–1751	ttgc**ag**/GTATCC	GGGCAG/**gt**gagg	12 (80)
**sv-c*	*intron 12 retained*		*GACCAA*/***gt****gagt*	
13 (171)	1752–1922	cttc**ag**/TTTGAC	GACCAA/**gt**gagt	13 (470)
14 (745)	1923–2651	cctc**ag**/AGGCCC		

[a] Numbering is based on the published cDNA sequence (19; U78294) with ATG starting at 72. The polyadenylation signal AATAA starting at 2651 was used as the last nucleotide of exon 14.
[b] The conserved intron-exon splice junctions (*i.e.* **gt** and **ag** in the introns) are in boldface type.
[c] The sizes of introns 3 and 5 could not be precisely determined due to their locations at the boundaries between sequencing clones. The size of intron 8 is based on Ref. 20 (AF149095).

TABLE III
Effect of 15(S)-HETE on prostate (cancer) cell proliferation and survival

NHP2, TP1, LNCaP, PC3, and Du145 cells were plated in 24-well culture plates at 1×10^4 cells/well. Next day cells were treated with 15(S)-HETE. NHP2 and TP1 cells were treated in their normal culture medium (see "Materials and Methods") and LNCaP, PC3, and Du145 cells were treated in RPMI 1640 medium supplemented with 2% FBS (instead of 5% FBS in their normal culture medium to reduce 15(S)-HETE binding to serum proteins). Seventy two h later, cells were harvested, and the number of live cells was determined using trypan blue dye exclusion assays (8). Each condition was run in quadruplicate, and the results are expressed as the mean % cell number (relative to vehicle (ethanol) control) ± S.E.

15(S)-HETE	NHP2	TP1	LNCaP	PC3	Du145
μM			*% control*		
0	100	100	100	100	100
1	102 ± 4	97 ± 9	123 ± 20	86 ± 3	62 ± 11
10	93 ± 6	72 ± 10	68 ± 9	63 ± 3	50 ± 4
25	64 ± 3	55 ± 5	50 ± 3	49 ± 3	37 ± 3
50	46 ± 3	27 ± 3	16 ± 5	34 ± 1	30 ± 4
75	30 ± 4	0	0	0	0

ably inhibits cell cycle progression. To test this possibility, we treated NHP2, TP1, LNCaP, PC3, and Du145 cells with 5, 10, and 25 μM 15(S)-HETE for 72 h. During the last 6 h, we pulsed the cells with 10 μM BrdUrd and analyzed cells in the S-phase by staining cells for BrdUrd incorporation (36, 42). As shown in Fig. 5*b*, 15(S)-HETE at 5 and 10 μM inhibited, in a concentration-dependent manner, BrdUrd incorporation in prostate cancer cells including TP1 cells, whereas NHP2 cells were completely resistant at these doses. At 25 μM, 15(S)-HETE inhibits cell cycle progression in all cells examined with TP1 cells being most sensitive (Fig. 5*b*).

We also analyzed the effects of several other related LOX products, namely 5(S)-HETE (a major 5-LOX product), 12(S)-HETE (the major 12-LOX product), and 13(S)-hydroxyoctadecadienoic acid (the major 15-LOX1 metabolite), on the same panel of cells. 5(S)-HETE induced significant cell death at as low as 1 μM and killed all cells at 10–25 μM, and 12(S)-HETE promoted proliferation of all cells, whereas 13(S)-hydroxyoctadecadienoic acid showed minimal effect up to 50 μM (not shown)

15-LOX2 Expression in NHP Cells Is Heterogeneous and Inversely Correlated with Cell Cycle Progression—To understand the biological function(s) of 15-LOX2, its expression was analyzed in NHP cells. To our surprise, 15-LOX2 expression in NHP2 (Fig. 6*a*), and NHP1 and NHP3 (not shown) cells was heterogeneous; some cells were strongly positive for 15-LOX2 expression and some weakly positive, whereas the majority of cells were negative. Overall, 12–20% of log-phase (passage 2–6) NHP (*i.e.* NHP1, NHP2, and NHP3) cells were positive for 15-LOX2 expression (not shown; also see Fig. 7*d*). The heterogeneous 15-LOX2 expression was seen even within clones; in a three-cell clone, for example, one cell was positive for 15-LOX2, whereas the other two were negative (Fig. 6*b*). In general, 15-LOX2-positive cells were larger than 15-LOX2-negative cells (Fig. 6, *a*, *b*, and *d*; also see Fig. 7). 15-LOX2 in positive NHP cells was homogeneously distributed as granules in the cytosol (Fig. 6, *b* and *d*). However, when a more harsh permeabilization/extraction method (*i.e.* acidic alcohol) was used, we found that a significant amount of 15-LOX2 was also localized to cell-cell borders and perinuclear regions (Fig. 6*c*). When we used the same protocols to stain PC3 and PPC-1 prostate cancer cells, we found no specific 15-LOX2 staining (not shown).

The heterogeneous nature of 15-LOX2 expression as well as the inhibitory effect of 15(S)-HETE on cell cycle (Fig. 5*b*) led us to think that 15-LOX2 expression in NHP cells may be normally coupled to cell cycle progression. To test this possibility, 15-LOX2 and BrdUrd double labeling studies were done. The results indeed revealed that although ~30% 15-LOX2$^-$ NHP2 cells were BrdUrd$^+$, <2% of 15-LOX2$^+$ cells were BrdUrd$^+$ (Fig. 6, *d* and *e*).

To explore further the relationship between 15-LOX2 expres-

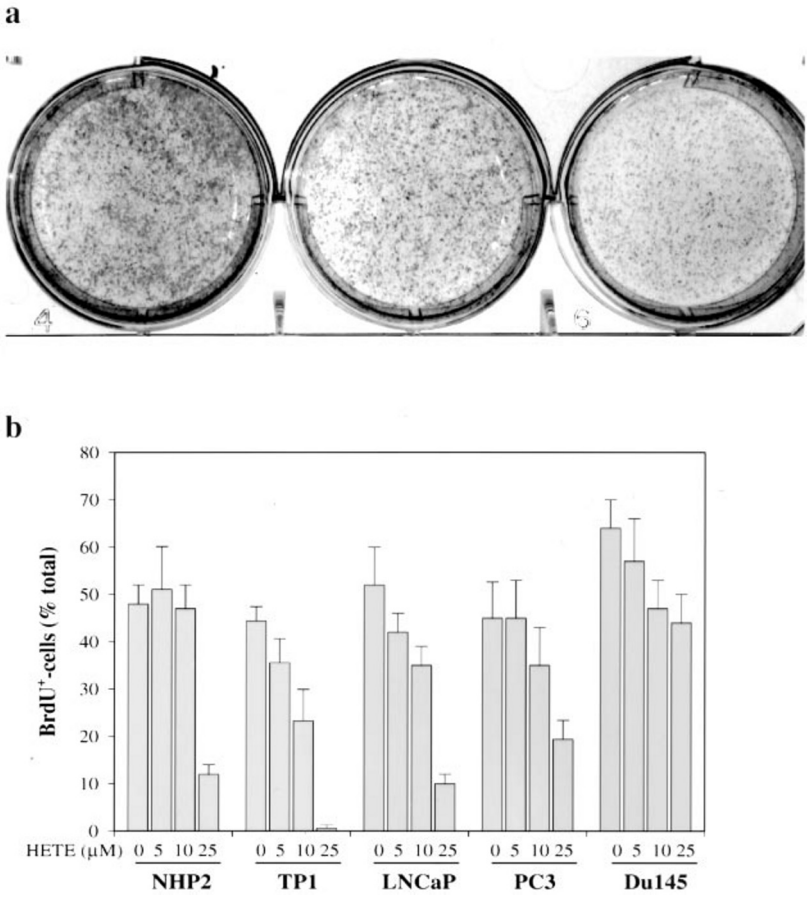

FIG. 5. **15(S)-HETE inhibits proliferation/survival of prostate cancer cells.** *a*, TP1 cells treated with 0 (*left*), 15 (*middle*), and 30 (*right*) μM 15(S)-HETE for 72 h. Cells were then stained with Giemsa, fixed, and photographed. *b*, 15(S)-HETE inhibits BrdUrd incorporation in prostate cancer cells. Various cells were treated with 15(S)-HETE at the doses indicated for 72 h. At the last 6 h, cells were pulsed with BrdUrd and then processed for BrdUrd staining. An average of 800–1000 cells were counted for each condition. The results are expressed as % BrdUrd$^+$ cells, and bars represent means ± S.E. derived from three independent experiments.

sion and cell cycle, we induced cell cycle arrest in NHP2 cells by culturing them in factor-free medium. In log-phase cultures (passages 2–6), ~13% NHP2 cells were 15-LOX2$^+$ (Fig. 7*d*), and 99% of these 15-LOX2$^+$ cells were BrdUrd$^-$ (Fig. 7*a* and data not shown). Among 15-LOX2$^-$ cells, ~32% were incorporating BrdUrd (Fig. 7*d*). Upon deprivation for 1 day, ~35% NHP2 cells became 15-LOX2$^+$ and, correspondingly, the % BrdUrd$^+$ cells dropped to <2% (Fig. 7, *b* and *d*). When starved NHP2 cells were re-cultured in normal factor-containing medium (*i.e.* released) for 1 day, the 15-LOX2$^+$ cells decreased to ~15%, and the BrdUrd$^+$ cells increased to ~35% (Fig. 7, *c* and *d*). Together, these data reinforce our earlier observations that 15-LOX2 expression is inversely correlated with cell cycle progression.

Restoration of 15-LOX2 in Prostate Cancer Cells Inhibits Cell Cycle Progression and Proliferation—To establish a cause-and-effect relationship between 15-LOX2 expression and cell cycle progression, we attempted to restore its expression in prostate cancer cells that have lost its expression (Fig. 1). To that end, we transiently transfected GFP-tagged expression vectors of 15-LOX2 and its splice variants into PPC-1 cells (because PPC-1 cells are most susceptible to liposome-mediated transfections) and, in some cases, PC3 cells and asked how this restoration of expression affects cell proliferation and/or death. Restoration of 15-LOX2 expression significantly reduced PPC-1 cell number, compared with transfection with vector alone (not shown). 15-LOX2sv-a also showed some although reduced inhibitory effect whereas 15-LOX2sv-b was much less inhibitory (not shown). The reduced cell number did not result from increased cell death, as we did not observe any obvious differences in apoptosis (ranging from 8 to 11%) between untransfected cells and cells transfected with control vector or 15-LOX2 expression vectors. Similar inhibitory effects on cell number were also observed in transfected PC-3 prostate cancer cells and 293 cells (not shown).

These results suggest that the inhibitory effect of 15-LOX2 likely resulted from an inhibition of cell cycle progression. We thus developed a modified BrdUrd labeling protocol that allowed us to detect cells in S-phase without jeopardizing the GFP signals (see "Materials and Methods"). This protocol also allowed us to directly compare the impact of restoring 15-LOX2 expression on cell cycle progression in isogenic populations of cells by comparing BrdUrd incorporation in GFP$^-$ *versus* GFP$^+$ cells. As shown in Fig. 8, GFP$^-$ and GFP$^+$-PPC-1 cells transfected with the control vector showed no difference in the % BrdUrd incorporation (~37%), which was slightly lower than that observed in untransfected cells (~42%). This low level of GFP cytotoxicity has been reported previously in other cell systems (43). In contrast, fewer GFP$^+$-PPC-1 cells transfected with 15-LOX2 (~15%) or 15-LOX2sv-a (~28%) were BrdUrd$^+$ compared with GFP$^-$ cells (~40%) (Figs. 8 and 9). By contrast, 15-LOX2sv-b demonstrated a much reduced inhibitory effect on PPC-1 cell BrdUrd incorporation (Fig. 8). The 15-LOX2 expression in the transfected cells was confirmed by immunostaining (Fig. 10). Experiments with a tri-color, double-labeling protocol (see "Materials and Methods") to simultaneously label 15-LOX2 and BrdUrd in GFP$^+$-cells revealed similar results (not shown).

DISCUSSION

The major findings of the present study are as follows: 1) 15-LOX2 is the major LOX expressed in NHP cells, which also express at least three 15-LOX2 splice variants; 2) 15-LOX2 protein expression is lost and its enzymatic activity greatly reduced in all prostate cancer cells examined; 3) loss of 15-LOX2 expression results from transcriptional repression via

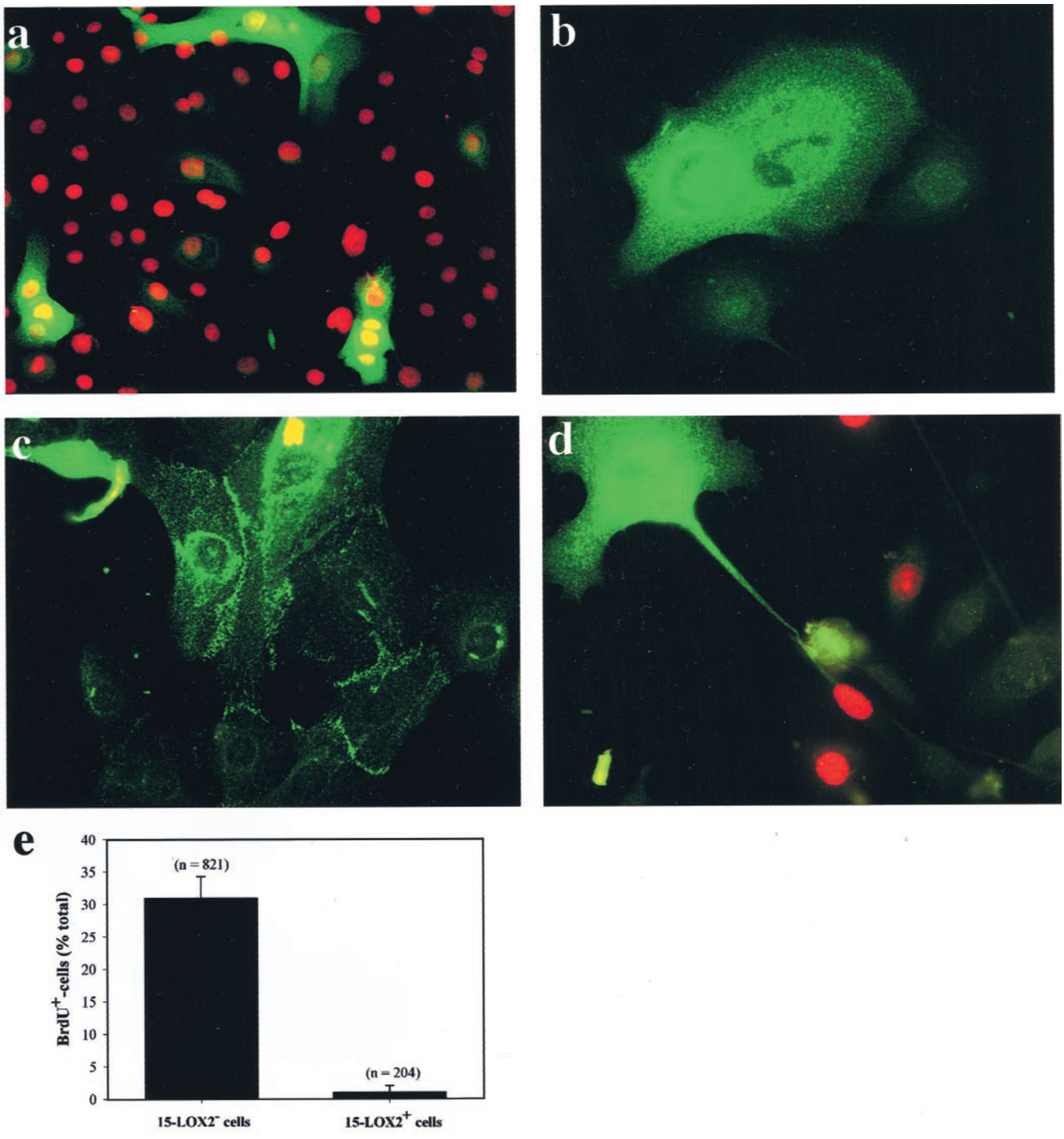

FIG. 6. **Heterogeneous 15-LOX2 expression and inverse correlation with cell cycle.** *a,* 15-LOX2 staining in log-phase NHP2 (passage 4) cells. Cell nuclei were counterstained with propidium iodide. Note that 15-LOX2 expression is heterogeneous in that some cells were strongly positive, some cells were weakly positive, and the majority of cells were negative for 15-LOX2 (*green*). *b*, intraclonal heterogeneity of 15-LOX2 expression. NHP cells (passage 5) were plated at clonal density (100 cells/13-mm^2 coverslip) and cultured for 3 days. Then the cells were used for 15-LOX2 immunostaining. Note that one cell is strongly positive for 15-LOX2, whereas the other two cells in the same clone were negative for 15-LOX2. *c*, localization of 15-LOX2 in cell-cell borders when cells were permeabilized/extracted with acidic alcohol. *d* and *e*, inverse correlation between 15-LOX2 expression and BrdUrd incorporation. The total number of cells counted was indicated in *e*. Magnifications: *a*, ×100; *b–d*, ×400.

mechanisms other than promoter hypermethylation or histone deacetylation-induced chromatin compaction; 4) 15-LOX2 product, 15(S)-HETE, preferentially inhibits cell cycle progression in prostate cancer cells; and 5) most importantly, 15-LOX2 expression in NHP cells is inversely correlated with cell cycle progression. Restoration of 15-LOX2 expression in prostate cancer cells induces cell cycle arrest. Together, these data provide strong evidence that 15-LOX2 may be an endogenous negative cell cycle regulator in NHP cells, which explains, in part, why it is advantageous for prostate cancer cells to suppress its expression.

NHP Cells Express Abundant 15-LOX2 and at Least Three Splice Variants—Several arachidonate LOXs, including 5-LOX, 12-LOX, and 15-LOX-1, have been reported to be upregulated in prostate cancer cells (see Introduction). 15-LOX2, by contrast, is the first LOX found to be expressed abundantly

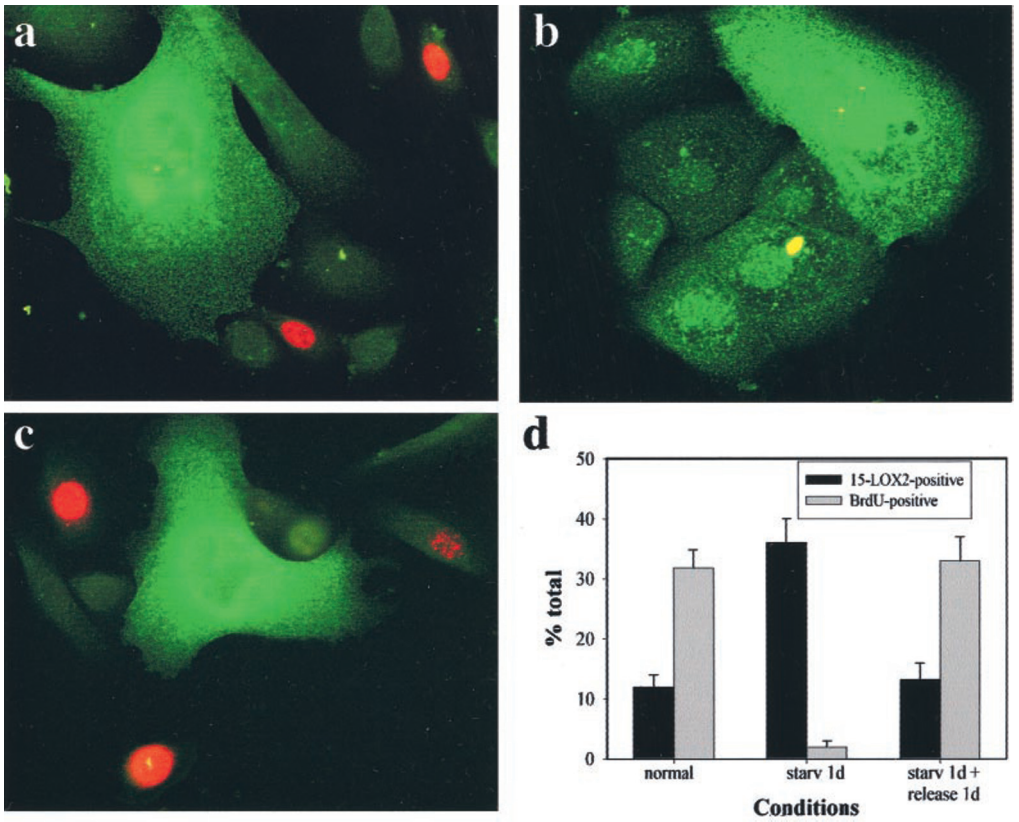

FIG. 7. **15-LOX2 expression is inversely correlated with cell cycle progression (*i.e. BrdUrd incorporation) in NHP2 cells.*** *a*, log-phase NHP2 (passage 4) cells double-labeled with 15-LOX2 (*green*) and BrdUrd (*red*). *b*, NHP2 cells deprived of growth factor for 1 day (starved 1 day) were double-labeled with 15-LOX2 (*green*) and BrdUrd (*red*). Note that none of the cells shown was incorporating BrdUrd. *c*, NHP2 cells starved for 1 day were released (*i.e.* re-cultured in factor-containing medium) for 1 day and then double-labeled with 15-LOX2 (*green*) and BrdUrd (*red*). Magnifications in *a–c*, ×400. *d*, quantification of 15-LOX2 expression and BrdUrd positivity (following a 4-h pulse) in NHP2 cells under various culture conditions. The results were means ± S.E. derived from two independent experiments. *starv 1d*, starved for 1 day.

in normal prostate but decreased or lost in prostate cancers *in vivo* (see Refs. 21 and 22 and see Supplemental Fig. 1). 15-LOX2 gene is localized on chromosome 17p13.1, a region where 12-LOX and 15-LOX1 genes also reside (44). 15-LOX2 gene consists of 14 exons (Table II; see Ref. 44), a structural organization similar to those of 5-LOX, 12-LOX, and 15-LOX1 (10, 11). Interestingly, 15-LOX2 has at least three splice variants. 15-LOX2sv-a, which is identical to the splice variant previously identified (20), is missing exon 9. Three-dimensional modeling of 15-LOX2sv-a structure, based on the crystallography data of 15-LOX1, suggests that a complete α-helix made of exon 9 is removed from the substrate-binding pocket (20). Therefore, 15-LOX2sv-a possesses reduced specific activity in metabolizing AA compared with 15-LOX2 (20). Consistent with its reduced enzymatic activity, we found that 15-LOX2sv-a also has a reduced biological (*i.e.* inhibiting BrdUrd incorporation) activity compared with 15-LOX2. Whether 15-LOX2sv-b and 15-LOX2sv-c have reduced enzymatic activities is currently under further investigation, although we did observe that the transfected 15-LOX2sv-b did not significantly inhibit the BrdUrd incorporation or cell proliferation (Fig. 8 and data not shown).

On Western blotting, we could variably detect three bands that migrate immediately below the 15-LOX2 band in NHP cells (*e.g.* Fig. 1 and Fig. 3*b*). Based on their relative molecular weight, these three bands may represent 15-LOX2sv-a, 15-LOX2sv-c, and 15-LOX2sv-b, respectively. These splice variants are generally expressed at much lower levels than 15-LOX2; with 1 μg of mRNA we could not detect their message (Fig. 2*b*), and their protein levels are also lower and variable (Fig. 1 and Fig. 3*b*). However, unlike 15-LOX2, these splice variants are still expressed in prostate cancer cells at variable

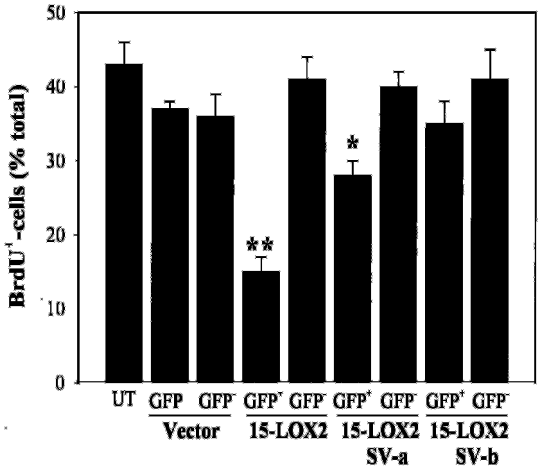

FIG. 8. **Restoration of 15-LOX2 expression in PPC-1 prostate cancer cells inhibits cell cycle progression.** PPC-1 cells were either untransfected or transfected with the control vector, pCMS-EGFP (control), or with various pEGFP-15-LOX2 expression vectors, *i.e.* 15-LOX2, 15-LOX2sv-a, and 15-LOX2sv-b. Seventy two h later, cells were pulsed with BrdUrd (for the last 4 h) and then processed for BrdUrd immunostaining. BrdUrd positivity was then scored in both GFP^- and GFP^+ cell populations under each condition. An average of 600–1500 cells was counted for each condition by two individuals, and the results are expressed as means ± S.E. derived from three to five independent experiments. **, $p < 0.05$; *, $p < 0.01$ compared with the vector-transfected cells.

levels. Interestingly, at least one more upper band and two other lower bands are also detected only in NHP but not in cancer cells (Fig. 1, *arrowheads*). Whether they also represent

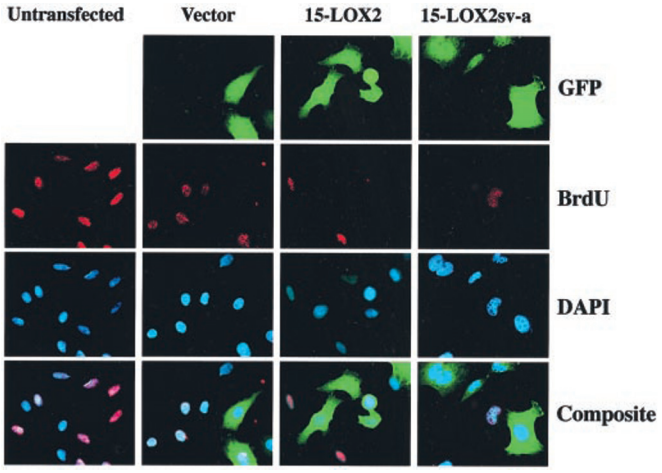

FIG. 9. **Restoration of 15-LOX2 expression in PPC-1 prostate cancer cells inhibits BrdUrd incorporation.** PPC-1 cells were either untransfected or transfected with the control vector, pCMS-EGFP (*Vector*), or with various pEGFP-15-LOX2 expression vectors, *i.e.* 15-LOX2, 15-LOX2sv-a, and 15-LOX2sv-b (not shown). Seventy two h later, cells were pulsed for the final 4 h with BrdUrd (10 μM) and then processed for BrdUrd immunostaining. All cell nuclei were counterstained with DAPI. Shown are representative micrographs showing that although some control vector-transfected cells were still incorporating BrdUrd most PPC-1 cells transfected with 15-LOX2 or 15-LOX2sv-a were not. See Fig. 8 for quantitative results. Original magnifications, ×200.

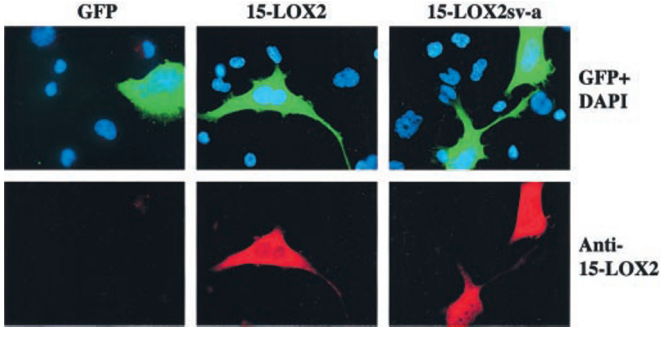

FIG. 10. **Micrographs showing that PPC-1 cells transfected with pEGFP-15-LOX2 or pEGFP-15-LOX2sv-a were stained positive for 15-LOX2 (*red*), and cells transfected with the control vector, pCMS-EGFP, were negative for 15-LOX2.** Similar positive staining was also observed in cells transfected with pEGFP-15-LOX2sv-b and pEGFP-15-LOX2sv-c (not shown). Original magnification, ×400.

15-LOX2 splice variants remains to be determined. When we performed PCR cloning with K-H primers, we detected several additional bands in addition to the three splice variants,[2] suggesting that there are probably more 15-LOX2 splice variants.

The biological functions of these splice variants are unclear. Like all other alternatively spliced products (45), they may help regulate and fine-tune the biological functions of the parental 15-LOX2. Because these splice variants have reduced enzymatic activities (20) but still can bind substrate (*i.e.* AA), it is conceivable that, under certain circumstances, they may function to "sink" AA so as to adjust the availability of AA to 15-LOX2.

15-LOX2 Expression Is Lost in All Prostate Cancer Cells Examined—That 15-LOX2 plays an important role in maintaining normal prostate homeostasis is also supported by the fact that prostate cancer cells lose its expression *in vivo* (21, 22) and *in vitro* (this study). The decrease or loss of 15-LOX2 expression in prostate cancer tissues occurs in the precursor lesion, high grade PIN (see Refs. 21 and 22 and Supplemental Fig. 1), suggesting that this may represent an early event in prostate tumorigenesis.

It is remarkable that all prostate cancer cells examined lost the expression of 15-LOX2. Even SV40-immortalized but non-transformed prostate epithelial cells lose 15-LOX2 expression.[3] Accompanying the loss of 15-LOX2 expression, prostate cancer cells also show reduced expression of 15-LOX2 splice variants. The decreased 15-LOX2 message (Fig. 4*a*) and protein (not shown) in TP1 primary carcinoma cells again suggest that suppression of 15-LOX2 expression may represent an early event in prostate tumorigenesis. The loss of 15-LOX2 protein expression leads to much less 15(S)-HETE production in prostate cancer cells compared with NHP cells (Table I). The low amount of 15(S)-HETE in prostate cancer cells may come from residual 15-LOX2 splice variants and/or 15-LOX1.

The loss of 15-LOX2 protein expression in cultured prostate cancer cells could result from transcriptional repression; Northern blotting fails to reveal and RT-PCR reveals only low levels or no 15-LOX2 mRNA expression in these cells (Fig. 2). Epigenetic gene silencing mechanisms, as a consequence of promoter hypermethylation and histone deacetylation-induced chromatin over-compaction, account for the transcriptional suppression of numerous mammalian (including some LOX) genes (37, 39, 46). For example, 15-LOX-1 expression in human colorectal carcinoma cells appears to be regulated by histone acetylation (46). However, these mechanisms do not seem to be responsible for the transcriptional silencing of 15-LOX2 in prostate cancer cells, as inhibitors of DNA methylation and/or HDAC could not relieve this suppression. Another potential mechanism for the loss of 15-LOX2 expression in prostate cancer cells is due to gene mutation, especially when considering that 15-LOX2 locus (17p13.1) is very close to p53 gene locus (17p13.2), which is frequently mutated in advanced prostate cancers (47). However, that suppression of 15-LOX2 protein expression occurs in precursor lesions (*i.e.* high grade PIN) and in primary carcinoma cells (TP1) casts some doubts on this possibility. 15-LOX1 mRNA expression is silenced during erythroid differentiation as a result of regulation at the 3′-untranslated region by heterogeneous nuclear ribonucleoproteins (48). Whether similar mechanisms involving RNA-binding proteins or transcription factors exist to silence the 15-LOX2 gene expression in prostate cancer cells is one of our ongoing research projects.

What Is the Biological Function of 15-LOX2?—Because 15-LOX2 is abundantly expressed in NHP cells but is lost in prostate cancer cells, the molecule may normally function by helping maintain the differentiated phenotype of prostate epithelial cells, restrict cell cycle progression, induce apoptosis of damaged or worn-out cells, or limit the migratory (or invasive) cellular behavior. These functions may not be mutually exclusive. One clue to 15-LOX2 function(s) comes from an analysis of the effect of its product, 15(S)-HETE, on prostate (cancer) cell proliferation and survival. At $\geq$25 μM, 15(S)-HETE induces apoptosis, and, at $<$25 μM, 15(S)-HETE reduces the number of cells in S-phase. 15(S)-HETE was recently shown to have a concentration-dependent inhibitory effect on colony formation of PC3 cells in soft agar with an IC_{50} at ~30 μM (23). This value is very similar to our data. It is unlikely that the 15(S)-HETE effect on prostate cancer cells is caused by nonspecific fatty acid cytotoxicity (9), because several other related eicosanoids tested show very different or even opposite effects. It is worth pointing out that the effective inhibitory dose(s) of 15(S)-HETE

[2] S. Tang and D. G. Tang, unpublished observations.

[3] B. Bhatia and D. G. Tang, unpublished observations.

on prostate cancer cells are high (Table I) (23). This is not very surprising because, very possibly, only a small fraction of 15(S)-HETE administered actually gets inside cells. Moreover, eicosanoids including 15(S)-HETE have been proposed to exert some of their biological functions through activating nuclear hormone receptors, peroxisome proliferator-activating receptors (PPAR), and the effective doses for eicosanoid activation of PPAR are at the 20–50 μM range (23, 49, 50). Therefore, if 15(S)-HETE is exerting its inhibitory effects on prostate cancer cells via PPARγ (23, 50), one would have to use high doses of this agonist. Cultured NHP cells produce ~30 ng of 15(S)-HETE/5 million cells when given exogenous AA (Table I), which corresponds to ~20 pmol of intracellular 15(S)-HETE/10^6 cells. Whether this concentration is high enough to produce any biological effect and how much endogenous 15(S)-HETE is produced by cultured NHP cells or NHP cells *in vivo* remain unknown. The biological function(s) of 15-LOX2, if mediated through its enzymatic activity, will be influenced by the availability of its substrate, AA. It is conceivable that under stimulated conditions both the concentration of free AA and the enzymatic activity of 15-LOX2 (20) may be up-regulated, leading to an increased 15(S)-HETE production and resultant cell cycle arrest and/or cell death.

Interestingly, NHP cells are more resistant to 15(S)-HETE-induced cell cycle arrest and apoptosis (Table III and Fig. 5*b*). This makes sense as these cells normally express abundant 15-LOX2 and produce endogenous 15(S)-HETE. This differential response may partially explain why prostate cancer cells lose 15-LOX2, because 15(S)-HETE is inhibitory to their clonal expansion. That TP1 primary carcinoma cells show more sensitive response than NHP2 cells, which are isolated from the same patient as TP1 cells (24), to 15(S)-HETE again supports the notion that decreased/lost 15-LOX2 expression and activity may represent an early molecular event during prostate tumorigenesis.

But what is the biological function(s) of 15-LOX2? Immunofluorescent staining surprisingly reveals that log-phase NHP cells heterogeneously express 15-LOX2, and this heterogeneity is even reflected among cells within one clone. Because most 15-LOX2$^+$ cells are larger than 15-LOX2$^-$ cells and also because 15(S)-HETE induces cell cycle arrest, we suspect that 15-LOX2 expression may be inversely correlated with cell cycle progression. Two lines of experiments subsequently confirmed this hypothesis. First, in log-phase NHP cell cultures, <2% 15-LOX2$^+$ cells are BrdUrd$^+$, whereas ~35% 15-LOX2$^-$ cells are BrdUrd$^+$. The very few 15-LOX2$^+$ cells that are BrdUrd$^+$ show low levels of 15-LOX2 expression, suggesting that perhaps 15-LOX2 protein expression has to reach a certain threshold to arrest cell cycle. Second, when NHP2 cells are subjected to starvation, there is an up-regulation in 15-LOX2 expression, from ~13 to 35%, and there is a corresponding decrease in the number of cells in S-phase, from ~35 to <2%. Although both sets of experiments do not establish whether it is the 15-LOX2 accumulation that arrests cell cycle or it is the cell cycle arrest that accumulates 15-LOX2, the observations do suggest that 15-LOX2 expression *is* correlated with cell cycle arrest. Because ~65% of NHP2 cells are not in cell cycle and only 13–20% of this population of cells express 15-LOX2, these results suggest that either 15-LOX2 expression is only one of the contributing factors in arresting cell cycle or, perhaps, 15-LOX2 protein is degraded before the cells are about to exit G_1.

Subsequent expression studies provide convincing evidence that 15-LOX2 expression does cause cell cycle arrest; restoration of 15-LOX2 expression in prostate cancer cells that have lost 15-LOX2 expression inhibits cell cycle progression and proliferation, leading to reduced cell number. 15-LOX2 overexpression in HEK 293, PPC-1, PC3, and Du145 cells for 3–5 days does not result in increased apoptosis. Even further overexpression of 15-LOX2 in NHP2 cells does not lead to apoptosis.[3] These observations suggest that, under unstimulated conditions, 15-LOX2 expression is not pro-apoptotic. This conclusion is consistent with the fact that NHP cells *in vivo* and *in vitro* express abundant 15-LOX2. This conclusion is also consistent with the effect of 15(S)-HETE, which only causes apoptosis when used at non-physiologically high concentrations. Together, these results suggest that, under basal conditions, perhaps only certain amounts of 15(S)-HETE can be produced, due to limited availability of AA, from either endogenous (in NHP cells) or exogenous (in transfected cancer cells) 15-LOX2 to help induce cell cycle arrest. These results also predict that, under stimulated conditions when increased AA becomes available, 15-LOX2 might cause cell apoptosis.

In summary, in this study we provide evidence that 15-LOX2 is a negative cell cycle regulator in normal prostate epithelial cells. Because normal adult prostate epithelial cells proliferate extremely slowly *in vivo* (47), the abundant expression of 15-LOX2 may help keep these cells in a relatively quiescent and differentiated state. That some 15-LOX2 also seems to localize to cell-cell borders (Fig. 6*c*) suggests that 15-LOX2 may also exert its biological functions via other mechanisms. Future studies will be directed toward understanding how 15-LOX2 (or its product) interacts with the cell cycle machinery and how prostate cancer cells suppress its expression.

Acknowledgment—We thank C. Conti for providing C4–2, C5, MDA 2a, and MDA 2b prostate cancer cells.

REFERENCES

1. Giovannucci, E., Rimm, E. B., Colditz, G. A., Stampfer, M. J., Ascherio, A., Chute, C. C., and Willett, W. C. (1993) *J. Natl. Cancer. Inst.* **85,** 1571–1579
2. Gann, P. H., Hennekens, C. H., Sacks, F. M., Grostein, F., Giovannucci, E. L., and Stampfer, M. J. (1994) *J. Natl. Cancer Inst.* **86,** 281–286
3. Wang, Y., Corr, J. G., Thaler, H. T., Tao, Y., Fair, W. R., and Heston, W. D. (1995) *J. Natl. Cancer Inst.* **87,** 1456–1462
4. Tang, D. G., Chen, Y., Diglio, C. A., and Honn, K. V. (1993) *J. Cell Biol.* **121,** 689–704
5. Han, J.-W., McCormick, F., and Macara, I. G. (1991) *Science* **251,** 204–207
6. Brash, A. R. (2001) *J. Clin. Invest.* **107,** 1339–1345
7. Tang, D. G., Porter, A. T., and Honn, K. V. (1997) *Adv. Exp. Med. Biol.* **407,** 405–411
8. Tang, D. G., Chen, Y. Q., and Honn, K. V. (1996) *Proc. Natl. Acad. Sci. U. S. A.* **93,** 5241–5246
9. Tang, D. G., La, E., Kern, J., and Kehrer, J. P. (2002) *Biol. Chem.* **383,** in press
10. Brash, A. R. (1999) *J. Biol. Chem.* **274,** 23679–23682
11. Kuhn, H., and Thiele, B. J. (1999) *FEBS Lett.* **449,** 7–11
12. Ghosh, J., and Myers, C. E. (1998) *Proc. Natl. Acad. Sci. U. S. A.* **95,** 13182–13187
13. Anderson, K. M., Seed, T., Vos, M., Mulshine, J., Meng, J., Alrefai, W., Ou, D., and Harris, J. E. (1998) *Prostate* **37,** 161–173
14. Gupta, S., Srivastava, M., Ahmad, N., Sakamoto, K., Bostwick, D. G., and Mukhtar, H. (2001) *Cancer* (*Phila.*) **91,** 737–743
15. Gao, X., Grignon, D. J., Chbihi, T., Zacharek, A., Chen, Y. Q., Sakr, W., Porter, A. T., Crissman, J. D., Pontes, J. E., Powell, I. J., and Honn, K. V. (1995) *Urology* **46,** 227–237
16. Nie, D., Tang, K., Diglio, C. A., and Honn, K. V. (2000) *Blood* **95,** 2304–2311
17. Spindler, S. A., Sarkar, F. H., Sakr, W. A., Blackburn, M. L., Bull, A. W., LaGattuta, M., and Reddy, R. G. (1997) *Biochem. Biophys. Res. Commun.* **239,** 775–781
18. Kelavkar, U. P., Cohen, C., Kamitani, H., Eling, T. E., and Badr, K. F. (2000) *Carcinogenesis* **21,** 1777–1787
19. Brash, A. R., Boeglin, W. E., and Chang, M. S. (1997) *Proc. Natl. Acad. Sci. U. S. A.* **94,** 6148–6152
20. Kilty, I., Alison, L., and Vickers, P. J. (1999) *Eur. J. Biochem.* **266,** 83–93
21. Shappell, S. B., Boeglin, W. E., Olson, S. J., Kasper, S., and Brash, A. R. (1999) *Am. J. Pathol.* **155,** 235–245
22. Jack, G. S., Brash, A. R., Olson, S. J., Manning, S., Coffey, C. S., Smith, J. A., Jr., and Shappell, S. B. (2000) *Hum. Pathol.* **31,** 1146–1154
23. Shappell, S. B., Gupta, R. A., Manning, S., Whitehead, R., Boeglin, W. E., Schneider, C., Case, T., Price, J., Jack, G. S., Wheeler, T. M., Matusik, R. J., Brash, A. R., and DuBois, R. N. (2001) *Cancer Res.* **61,** 497–503
24. Chopra, D. P., Grignon, D. J., Joiakim, A., Mathieu, P. A., Mohamed, A., Sakr, W. A., Powell, I. J., and Sarkar, F. H. (1996) *J. Cell. Physiol.* **169,** 269–280
25. Chopra, D. P., Sarkar, F. H., Grignon, D. J., Sakr, W. A., Mohamed, A., and Waghray, A. (1997) *Cancer Res.* **57,** 3688–3692
26. Tang, D. G., Li, L., Chopra, D., and Porter, A. T. (1998) *Cancer Res.* **58,** 3466–3479
27. Brothman, A. R., Wilkins, P. C., Sales, E. W., and Somers, K. D. (1991) *J. Urol.* **145,** 1088–1091

28. Navone, N. M., Olive, M., Ozen, M., Davis, R., Tronsco, P., Tu, S.-M., Johnston, D., Pollack, A., Pathak, S., von Eschenbach, A. C., and Logothetis, C. J. (1997) *Clin. Cancer Res.* **3,** 2493–2500
29. Horoszewicz, J. S., Leong, S. S., Kawinski, E., Karr, J. P., Rosenthal, H., Chu, T. M., Mirand, E. A., and Murphy, G. P. (1983) *Cancer Res.* **43,** 1809–1818
30. Wu, H.-C., Hsieh, J.-T., Gleave, M. E., Brown, N. M., Pathak, S., and Chung, L. W. K. (1994) *Int. J. Cancer* **57,** 406–412
31. Kaighn, M. E., Narayan, K. S., Ohnuki, Y., Lechner, J. F., and Jones, L. W. (1979) *Investig. Urol.* **17,** 16–23
32. Stone, K. R., Mickey, D. D., Wunderli, H., Mickey, G. H., and Paulson, D. F. (1978) *Int. J. Cancer* **21,** 274–281
33. Muraki, J., Addonizio, J. C., Choudhury, M. S., Fischer, J., Eshghi, M., Davidian, M. M., Shapiro, L. R., Wilmot, P. L., Nagamatsu, G. R., and Chiao, J. W. (1990) *Investig. Urol.* **36,** 79–84
34. Iizumi, T., Yazaki, T., Kanoh, S., Kondo, I., and Koiso, K. (1987) *J. Urol.* **137,** 1304–1306
35. Kempen, E. C., Yang, P., Felix, E., Madden, T., and Newman, R. A. (2001) *Anal. Biochem.* **297,** 183–190
36. Tang, D. G., Tokumoto, Y. M., and Raff, M. C. (2000) *J. Cell Biol.* **148,** 971–984
37. Jones, P. A., and Takai, D. (2001) *Science* **293,** 1068–1070
38. Yoshida, M., Kijima, M., Akita, M., and Beppu, T. (1990) *J. Biol. Chem.* **268,** 17174–17179
39. Jenuwein, T., and Allis, C. D. (2001) *Science* **293,** 1074–1080
40. Tang, D. G., Tokumoto, Y. M., Apperly, J., Lloyd, A. C., and Raff, M. C. (2001) *Science* **291,** 868–871
41. Scheffler, I. E. (1999) *Mitochondria,* pp 89–103, Wiley-Liss, Inc., New York
42. Maguad, J. P., Sargent, I., and Mason, D. Y. (1988) *J. Immunol. Methods* **106,** 95–100
43. Endow, S. A., and Piston, D. W. (1998) in *Green Fluorescent Protein: Properties, Applications, and Protocols* (Chaltrie, M., and Kain, S., eds) p. 288, Wiley-Liss, Inc., New York
44. Krieg, P., Marks, F., and Furstenberger, G. (2001) *Genomics* **73,** 323–330
45. Lopez, A. J. (1998) *Annu. Rev. Genet.* **32,** 279–305
46. Kamitani, H., Taniura, S., Ikawa, H., Watanabe, T., Kelavkar, U., and Eling, T. E. (2001) *Carcinogenesis* **22,** 187–191
47. Abate-Shen, C., and Shen, M. M. (2000) *Genes Dev.* **14,** 2410–2434
48. Ostarek, D. H., Ostarek-Lederer, A., Shatsky, I. N., and Hentze, M. W. (2001) *Cell* **104,** 281–290
49. Kersten, S., Desvergne, B., and Wahli, W. (2000) *Nature* **405,** 421–424
50. Huang, J. T., Welch, J. S., Ricote, M., Binder, C. J., Wilson, T. M., Kelly, C., Witztum, J. L., Funk, C. D., Conrad, D., and Glass, C. K. (1999) *Nature* **400,** 378–382